Changes in firing pattern of lateral geniculate neurons caused by membrane potential dependent modulation of retinal input through NMDA receptors

S. Augustinaite[1,2] and P. Heggelund[1]

[1] *Institute of Basic Medical Sciences, Department of Physiology, University of Oslo, PO Box 1103 Blindern, N-0317 Oslo, Norway*
[2] *Department of Biochemistry and Biophysics, Faculty of Natural Sciences, Vilnius University, Ciurlionio 21, 03101 Vilnius, Lithuania*

An optimal visual stimulus flashed on the receptive field of a retinal ganglion cell typically evokes a strong transient response followed by weaker sustained firing. Thalamocortical (TC) neurons in the dorsal lateral geniculate nucleus, which receive their sensory input from retina, respond similarly except that the gain, in particular of the sustained component, changes with level of arousal. Several lines of evidence suggest that retinal input to TC neurons through NMDA receptors plays a key role in generation of the sustained response, but the mechanisms for the state-dependent variation in this component are unclear. We used a slice preparation to study responses of TC neurons evoked by trains of electrical pulses to the retinal afferents at frequencies in the range of visual responses *in vivo*. Despite synaptic depression, the pharmacologically isolated NMDA component gave a pronounced build-up of depolarization through temporal summation of the NMDA receptor mediated EPSPs. This depolarization could provide sustained firing, the frequency of which depended on the holding potential. We suggest that the variation of sustained response *in vivo* is caused mainly by the state-dependent modulation of the membrane potential of TC neurons which shifts the NMDA receptor mediated depolarization closer to or further away from the firing threshold. The pharmacologically isolated AMPA receptor EPSPs were rather ineffective in spike generation. However, together with the depolarization evoked by the NMDA component, the AMPA component contributed significantly to spike generation, and was necessary for the precise timing of the generated spikes.

(Received 2 March 2007; accepted after revision 10 May 2007; first published online 10 May 2007)
Corresponding author P. Heggelund: University of Oslo, Institute of Basic Medical Sciences, Department of Physiology, PO Box 1103 Blindern, N-0317 Oslo, Norway. Email: paul.heggelund@medisin.uio.no

A major function of thalamic relay nuclei is state-dependent regulation of input to cortex. Accordingly the response pattern of thalamocortical (TC) neurons to a given primary afferent input varies with states of the individual. Well-known examples are the state-dependent shifts in the visual response of TC neurons in the dorsal lateral geniculate nucleus (LGN) which transfers signals from retinal ganglion cells to neurons in visual cortex. In retinal ganglion cells an optimal visual stimulus flashed on the receptive field centre typically evokes a strong transient response followed by weaker sustained firing. TC neurons in LGN show a similar response pattern except that the balance between the transient and the sustained response component varies in a state-dependent manner. In conditions characteristic of drowsiness or non-REM sleep, the sustained response is weak and the initial transient dominates the firing pattern. During arousal, there is an increased firing rate that is most pronounced in the sustained response component (Hubel, 1960; Livingstone & Hubel, 1981; Francesconi *et al.* 1988; Funke & Eysel, 1992, 2000; Humphrey & Saul, 1992; Hartveit & Heggelund, 1992, 1993, 1995; Funke *et al.* 1993; Hartveit *et al.* 1993; Li *et al.* 1999; Fjeld *et al.* 2002). Another example is the shift in spontaneous activity from burst firing in slow-wave sleep to more regular firing in awake states (Hubel, 1960; Livingstone & Hubel, 1981). The burst firing is caused by rhythmic low-threshold calcium spikes (Deschênes *et al.* 1982, 1984; Jahnsen & Llinas, 1984*a*,*b*; Steriade & Deschênes, 1984) at the hyperpolarized membrane potentials that typically occur in slow-wave sleep. The shift to regular firing occurs by depolarization that inactivates T-channel calcium conductances (Hirsch *et al.* 1983; Deschênes *et al.* 1982, 1984; Jahnsen & Llinas, 1984*a*,*b*; Crunelli *et al.* 1989; McCormick & Pape, 1990; Curró Dossi *et al.* 1991). The mechanisms for the shift from transient to sustained firing are less well known. Rather than being due to intrinsic calcium conductances in the TC neurons, this change

 DOI: 10.1113/jphysiol.2007.131540

seems to be related to mechanisms of retinogeniculate synaptic transmission.

The retinal input to TC neurons is mediated by both NMDA receptors (NMDA-Rs) and non-NMDA-Rs (Hartveit & Heggelund, 1990; Heggelund & Hartveit, 1990; Scharfman *et al.* 1990; Sillito *et al.* 1990*a*,*b*; Funke *et al.* 1991; Turner *et al.* 1994). *In vivo* studies have suggested that the NMDA-Rs play a particularly important role in this type of synapse (Heggelund & Hartveit, 1990; Sillito *et al.* 1990*b*). The non-NMDA-Rs are of the AMPA type (Kielland & Heggelund, 2001; Chen *et al.* 2002). AMPA receptors (AMPA-Rs) have approximately linear voltage dependence (Hestrin *et al.* 1990), their EPSCs have a fast rise-time, lasting for milliseconds (Turner *et al.* 1994), and they may elicit short-latency spikes which preserve the timing of the afferent spikes (Blitz & Regehr, 2003). NMDA-Rs have highly non-linear voltage dependence (Mayer *et al.* 1984; Nowak *et al.* 1984), their EPSCs have slower rise-time, lasting for tens of milliseconds (Turner *et al.* 1994), and they elicit longer-latency spikes with more variable timing with reference to afferent spikes (Blitz & Regehr, 2003). By repetitive stimulation, both the AMPA and NMDA components show synaptic depression due to presynaptic mechanisms, and different post-synaptic mechanisms: fast desensitization of AMPA-Rs and saturation of NMDA-Rs (Chen *et al.* 2002; Kielland & Heggelund, 2002).

Several lines of evidence are consistent with the hypothesis that the sustained firing of TC neurons during static visual stimulation depends on input mediated by NMDA-Rs. *In vivo* experiments (Hartveit & Heggelund, 1990; Heggelund & Hartveit, 1990; Funke *et al.* 1991) have shown that NMDA-R antagonists strongly attenuate the sustained response in TC neurons of the non-lagged class (Mastronarde, 1987*a*), whereas the effect on the initial transient response is less consistent. In the class of lagged cells (Mastronarde, 1987*a*), which lack the initial transient and only give a relatively sustained response, NMDA-R antagonists almost completely abolish the visual response (Heggelund & Hartveit, 1990). Consistent with this, the timing of spikes in lagged cells is considerably less precise with reference to spikes in the retinal afferents than the timing in non-lagged cells (Mastronarde, 1987*b*). In line with these findings, *in vitro* studies have demonstrated that sustained spike firing in TC neurons during train stimulation of retinal afferents largely depends on input mediated through NMDA-Rs (Turner *et al.* 1994; Blitz & Regehr, 2003).

The non-linear voltage dependence of the NMDA-Rs is due to a Mg^{2+} blockade that is pronounced at hyper-polarized membrane potentials but gradually relieved by increasing membrane depolarization (Mayer *et al.* 1984; Nowak *et al.* 1984). Accordingly, in states when the TC neurons become depolarized, the NMDA component during repetitive inputs might become more pronounced and could reach the threshold for spike generation through temporal summation of the EPSPs. Thus, modulation of the membrane potential that adjusts the effect of the NMDA component could be a key mechanism for regulation of the degree of sustained firing during visual stimulation *in vivo*, and during train stimulation *in vitro*. Depolarization in the intact animal might be evoked by modulatory input from state-related nuclei in the brainstem (McCormick, 1992; Steriade *et al.* 1997), excitatory feedback from cortex (Lindström & Wróbel, 1990; Turner & Salt, 1998; von Krosigk *et al.* 1999), and possibly also strong input from retina. However, the pronounced synaptic depression at the retinogeniculate synaptic transmission (Chen *et al.* 2002; Kielland & Heggelund, 2002), might prevent generation of a sufficiently strong NMDA component. This raises the question of how NMDA-R mediated EPSPs in TC neurons summates temporally during repetitive retinal input at different membrane potentials.

To address this question, we made whole-cell recordings in current clamp and studied how responses of TC neurons to train stimulation of retinal afferents varied depending on the holding potential of the neuron. We used train stimuli with frequencies characteristic for responses of retinal ganglion cells to visual stimuli *in vivo* (Balkema & Pinto, 1982; Stone & Pinto, 1992). The response of the TC neurons to afferent stimulation is determined by several other factors beside the retinogeniculate synaptic input, like intrinsic conductances of the TC cell, inhibitory inputs, excitatory cortical feedback, and modulatory brainstem input (McCormick, 1992; Steriade *et al.* 1997). In the present study we were interested in properties of the retinogeniculate synaptic transmission, which is a basic factor in determining responses of TC neurons. We therefore used a preparation in which other inputs were eliminated or pharmacologically blocked. The separate NMDA and AMPA components of the retinogeniculate inputs were isolated pharmacologically. We found that the isolated NMDA component gave an increasing depolarization through temporal summation of EPSPs during train stimulation, despite the synaptic depression. This depolarization could provide sustained firing of the neuron with a frequency that depended on the holding potential. The isolated AMPA component was rather ineffective for spike generation. When the pulse train was delivered without immediately preceding synaptic input, the AMPA component could elicit short-latency spiking at the beginning of the train. However, when a few pulses of lower frequency, typical for maintained firing of retinal ganglion cells *in vivo* (Balkema & Pinto, 1982; Stone & Pinto, 1992), preceded this pulse train, sufficient depression was generated to abolish the initial spiking. Together with the depolarization evoked by the NMDA component, the AMPA component contributed significantly to spike generation, and the

AMPA component was necessary for precise timing of the spikes with respect to the timing of the afferent pulses. The relationship between the degree of NMDA-R mediated sustained firing and the holding potential demonstrated that the degree of sustained response would be very sensitive for state-dependent regulations of the membrane potential of the TC neuron. We suggest that regulation of the sustained response through the level of the membrane potential is a key mechanism for regulation of the strength of input to cortex depending on states like arousal, attention and vigilance, a regulation that can be controlled from both cortex and the brainstem.

Methods

Experiments were performed in brain slices prepared from C57BL/6 mice. The preparation was done according to the guidelines, and with the approval, of the Animal Care Committee in Norway. Animals, 17–21 days old, were deeply anaesthetized with isoflurane and killed by rapid decapitation. A block of the brain was dissected out and cooled to ∼4°C in artificial cerebrospinal fluid (ACSF) containing (mM): 125 NaCl, 25 $NaHCO_3$, 2.5 KCl, 2 $CaCl_2$, 1.25 NaH_2PO_4, 1 $MgCl_2$, 25 D-glucose, and bubbled with 5% CO_2–95% O_2. Brain slices of LGN were cut from the block at a thickness of 250 μm, in a semiparasagittal plane, as previously described (Turner & Salt, 1998), using a vibroslicer (Sigmann Electronics, Hüffenhardt, Germany). The slices were stored submerged in ACSF at 30°C until recording, and were used within 4 h.

During experiments, slices were kept submerged in a small chamber (volume, ∼1.5 ml). The chamber was perfused with ACSF at the rate of 3 ml min^{-1} at a temperature of 36°C using an inline heater. In all experiments picrotoxin (50 μM; Sigma-Aldrich, St Louis, MO, USA) was added to the perfusion solution to block $GABA_A$ synaptic inputs. CGP54626 hydrochloride (5 μM; Tocris Bioscience, Bristol, UK) was added to block $GABA_B$ effects elicited by repetitive stimulation of retinal afferents (Soltesz & Crunelli, 1992). A selective $GABA_C$ receptors antagonist was not added because in the feed-forward inhibitory loop, which could be activated by our stimulation of retinal afferents, all IPSPs seems to be blocked by $GABA_A$ and $GABA_B$ antagonists (Perreault *et al.* 2003; Blitz & Regehr, 2005). We added 2,3-dioxo-6-nitro-1,2,3,4-tetrahydrobenzo[f]quinoxaline-7-sulphonamine disodium salt (NBQX; 10 μM; Tocris Bioscience, Bristol, UK) and (*RS*)-3-2-carboxypiperazin-4-yl-propyl-1-phosphonic acid (CPP; 10–15 μM; Tocris Bioscience, Bristol, UK) to the perfusion solution, as indicated, to block AMPA and NMDA receptors, respectively. We used NBQX to block AMPA-Rs. Although NBQX is a non-NMDA-R antagonist that blocks kainate receptors in addition to AMPA receptors (Sheardown *et al.* 1990), it has been shown that the non-NMDA receptors at the retinogeniculate synapses are of the AMPA type (Kielland & Heggelund, 2001; Chen *et al.* 2002).

Whole cell current-clamp recordings were made from TC neurons in LGN. The cells were visualized with differential interference contrast microscopy using infrared light. TC neurons were distinguished from local interneurons by their morphological (rounded soma and three or more primary dendrites; Zhu *et al.* 1999) and physiological characteristics (lower input resistance and shorter membrane time constant; Perreault *et al.* 2003). Recordings were obtained with borosilicate glass electrodes (4–6 MΩ) filled with (mM): 115 potassium gluconate, 20 KCl, 10 Hepes, 2$MgCl_2$, 2 MgATP, 2 Na_2ATP, 0.3 GTP. The pH was adjusted to 7.3 with KOH. In some of the experiments, as indicated, 2-[(2,6-dimethylphenol)amino]-*N*,*N*,*N*-trimethyl-2-oxoethanaminium chloride (QX 222; 4–6 mM; Tocris Bioscience, Bristol, UK) was included in the intracellular solution to block Na^+ action potentials. The electrical signals were amplified and low-pass filtered at 10 kHz with an Axoclamp 2A amplifier (Molecular Devices, Palo Alto, CA, USA) and Pulse software (HEKA Elektronik, Lambrecht, Germany). Bridge-balance circuitry was used to compensate for electrode resistance. Capacitance neutralization was used to compensate for membrane capacitance. Compensations and series resistances (< 20 MΩ) were checked periodically throughout the experiment. Data were digitized at 10 kHz with an ITC-18 interface (Instrutech, Port Washington, NY, USA).

Excitatory postsynaptic potentials (EPSPs) in TC neurons were evoked by electrical stimulation of retinogeniculate fibres with bipolar electrodes, using 100 μs-long current pulses. For each neuron the current strength was increased to a value (10–200 μA) at which it evoked an action potential to a single pulse at a holding potential of −55 mV, and kept at this value throughout the recordings from a given neuron. Stimulus protocols were pulse trains of 10 pulses at 50, 80 or 100 Hz, which are in the range of spike firing of mouse retinal ganglion cells to visual stimuli *in vivo* (Balkema & Pinto, 1982; Stone & Pinto, 1992). The membrane potential of the neurons was adjusted to different steady state values in the range between −60 and −45 mV by constant current injection through the recording electrode. For each experimental condition, responses to 5–10 repetitive stimulus presentations were recorded with 20 s intervals between presentations (30 s for experiments with three-parted stimulus trains). Spike latency was calculated as time from stimulus pulse to peak of action potential.

Offline data analyses were made with Igor Pro (Wave Metrics, Lake Oswego, OR, USA). Statistical analyses were performed with Igor Pro and Statistica (StatSoft, Inc., Tulsa, OK, USA). Results are given as means ± S.E.M. The statistical difference between groups was determined using the Friedman ANOVA test.

Results

Whole cell current clamp recordings were made from TC neurons in thalamic slices cut in a pseudo parassagittal plane in which optic tract fibres were preserved (Turner & Salt, 1998). The recordings were made at physiological temperature (36°C). Since our focus was on the retinal synaptic input to TC neurons, we blocked $GABA_A$ and $GABA_B$ receptors by antagonists added to the bath solution. We studied responses in TC neurons ($n = 46$) evoked by electrical pulse trains to retinal afferents with frequencies in the range of 50–100 Hz. This is within the range of normal firing rate to visual stimulation of mouse retinal ganglion cells *in vivo* (Balkema & Pinto, 1982; Stone & Pinto, 1992). The input resistance of the cells varied between 149 and 292 MΩ (mean, $m = 198$, s.d. = 40.7 MΩ, $n = 42$), and the time constant varied between 22.4 and 45.7 ms ($m = 32.9$, s.d. = 6.9 ms, $n = 42$); values that are within the range for TC neurons (Perreault *et al.* 2003). The resting membrane potential of the cells in the control condition without afferent stimulation varied across cells from −68 to −55 mV ($m = -63.9$ mV, s.d. = 3.2, $n = 46$). The membrane potential of the neurons was adjusted to different values in the range between −60 and −45 mV by constant current injection through the recording electrode. We studied changes of response patterns across these different holding potentials.

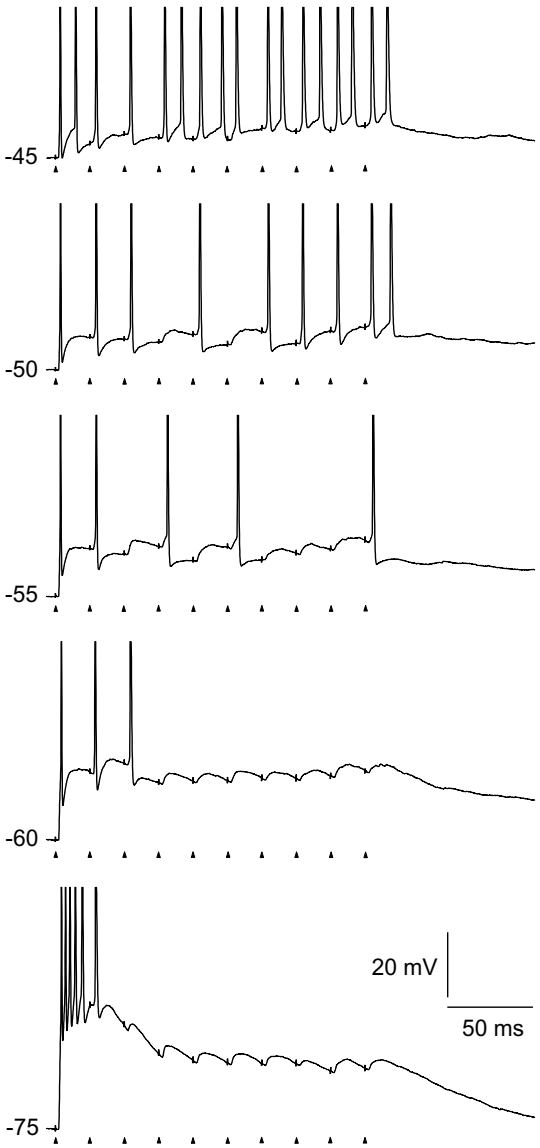

Figure 1. Firing patterns of a TC neuron at different holding potentials evoked by pulse train stimulation of retinal afferents
The frequency of the pulse train was 50 Hz. Holding potentials are indicated to the left of the trace. Timing of stimulus pulses is indicated by arrow-heads below the traces, and can also be deduced from the stimulation artefacts on the traces (truncated). Spike amplitudes were truncated at 0 mV.

Firing pattern at different holding potentials

The firing pattern to train stimulation changed with the setting of holding potential with respect to both the number of spikes and to which pulses in the train that elicited a spike. The typical variation of firing pattern is illustrated by the traces in Fig. 1. At −75 mV, as expected, the pattern was dominated by a short-latency low-threshold calcium potential, and the elicited action potentials lacked precise timing with respect to the single pulses in the stimulus train, consistent with previous findings (Blitz & Regehr, 2003). At normal resting potential (−60 mV), only the first one to three pulses of the train generated a spike. At the more depolarized holding potentials, spikes were generated also in the later part of the train, with increasing number as the holding potential was shifted to more depolarized levels.

To study the contribution of the AMPA and NMDA components to the firing pattern, we isolated these components pharmacologically. Since we were primarily interested in changes of sustained firing during the stimulus trains, we focused on firing patterns at holding potentials depolarized above −60 mV, conditions at which the T-calcium conductances are completely or almost completely inactivated. For control recordings of response pattern before wash-in of receptor antagonists we used a holding potential of −50 mV, a holding potential at which both the NMDA and AMPA components were relatively strong.

To study the contribution of the AMPA component we blocked the NMDA-Rs by adding the selective antagonist CPP to the bath solution. At a holding potential of −50 mV, this abolished all spikes except those to the very first pulses of the train (Fig. 2*B*). To study the contribution of the NMDA component, we blocked AMPA-Rs by application of NBQX. This selectively abolished the spikes at the

beginning of the stimulation with less marked effects on the number of spikes in the later part of the train (Fig. 2*D*). This is consistent with previous *in vivo* and *in vitro* experiments suggesting that the NMDA component is necessary for firing during the later parts of a stimulus (Salt, 1987; Hartveit & Heggelund, 1990; Heggelund & Hartveit, 1990; Funke *et al.* 1991; Zhang & Kelly, 2001; Blitz & Regehr, 2003).

In most cells it was difficult to wash-out the effects of the receptor antagonists completely. Thus, rather than comparing the effects of NMDA-R and AMPA-R antagonists on the same neuron, which could give distorted results due to incomplete washout, we mainly studied the effects of the two antagonists on different cells ($n = 40$). The effects of NMDA-R antagonists were studied on 23 cells, and the effects of AMPA-R antagonists on 17 cells.

Temporal summation of EPSPs at different holding potentials

The firing patterns shown in Fig. 2 suggest that the temporal summation of EPSPs during the train stimulus is markedly different for the AMPA and NMDA components. We determined the temporal summation of EPSPs of the two components separately, and studied how they changed with variation of the holding potential. To determine the summation without distortions from action potentials and the subsequent after-hyperpolarization, we blocked the voltage-dependent sodium channels by adding QX222 to the intracellular solution ($n = 27$). The NMDA component was studied in 17 neurons, the AMPA component in 10 neurons.

The temporal summation of the EPSPs of the NMDA component gave gradually increasing depolarization during the stimulus trains at all holding potentials, despite the synaptic depression of the NMDA-R (Chen *et al.* 2002; Kielland & Heggelund, 2002). This is illustrated by the example in Fig. 3*A*. The black traces show the summation of the isolated NMDA component. The grey traces show the summation of EPSPs mediated by both AMPA and NMDA components in the control condition before wash-in of NBQX. Clearly, the single EPSPs elicited by the NMDA component had a relatively long duration compared with the interpulse intervals at 50 Hz. However, the increment of depolarization from one EPSP to the next decreased during the pulse train such that the sum gradually levelled out towards a plateau as expected from increasing synaptic depression during the pulse train. It is evident from the traces that the neuron would reach the threshold for spike firing at different parts of the pulse train depending on the underlying membrane potential.

The typical temporal summation pattern of the EPSPs of the isolated AMPA component is illustrated in Fig. 3*B* (black traces). The first pulse of the train stimulus generated a large EPSP at each holding potential tested. The amplitude of the subsequent EPSPs gradually decreased, such that the temporal summation gave decreasing depolarization towards a plateau, consistent with the fast depression of the AMPA-Rs (Chen *et al.* 2002; Kielland & Heggelund, 2002), and the short duration of the single EPSPs.

The depolarization elicited by the NMDA and AMPA components complemented each other, such that at the beginning of the train when the NMDA component was weak, the AMPA component was strong, and in the subsequent parts when the AMPA component declined, the NMDA component increased. Thus, the combination of the two components (grey traces in Fig. 3) provided strong depolarization throughout the pulse train.

For the neuron illustrated in Fig. 3*A*, the depolarization accumulated during the train by the NMDA component

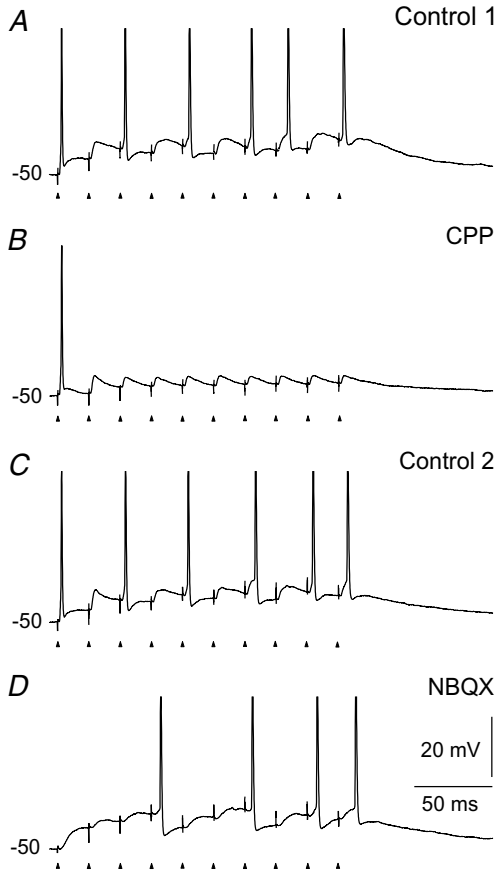

Figure 2. Contributions of AMPA and NMDA components to the firing patterns evoked by stimulation of retinal afferents
The frequency of the pulse train was 50 Hz. *A*, response in the control condition before application of the NMDA receptor antagonist CPP. *B*, firing pattern mediated by the AMPA component after application of 10 μM CPP through the perfusion solution. *C*, response after wash-out of CPP. *D*, firing pattern mediated by the NMDA component after blockade of the AMPA-Rs by 10 μM NBQX.

was largest at a holding potential of −60 mV, and decreased gradually as the holding potential was shifted to more depolarized level. However, this was not the case for all of the neurons tested ($n = 10$). For most of them the accumulated depolarization was about the same at all four holding potentials, as illustrated for three neurons in Fig. 4. However, the degree of accumulated depolarization at the end of the pulse train differed considerably from neuron to neuron in the range from 5.1 mV to 18.6 mV ($m = 11.4 \pm 0.6$ mV).

For each of the neurons illustrated in Figs 3*A* and 4, the slope at the beginning of the response traces became steeper as the holding potential was shifted to more depolarized levels. Thus, the initial increase of depolarization was faster at the more depolarized holding potentials. To test this for all neurons we fitted exponentials to the traces. A single exponential could not adequately fit any of the curves. We therefore used double exponential functions (dashed lines in Fig. 4) with a fast time constant describing the response at the beginning of the train. The average of this fast constant changed from 44.5 ± 7.3 ms at −60 mV to 15.8 ± 1.6 ms at −45 mV ($P < 0.0001$, d.f. = 3; $n = 10$).

The rather large standard error at −60 mV could be due to a variable residual contribution of T-type calcium current that can occur at this membrane potential (Crunelli *et al.* 2005). This was confirmed for two neurons in which we found a minor reduction of the EPSP to

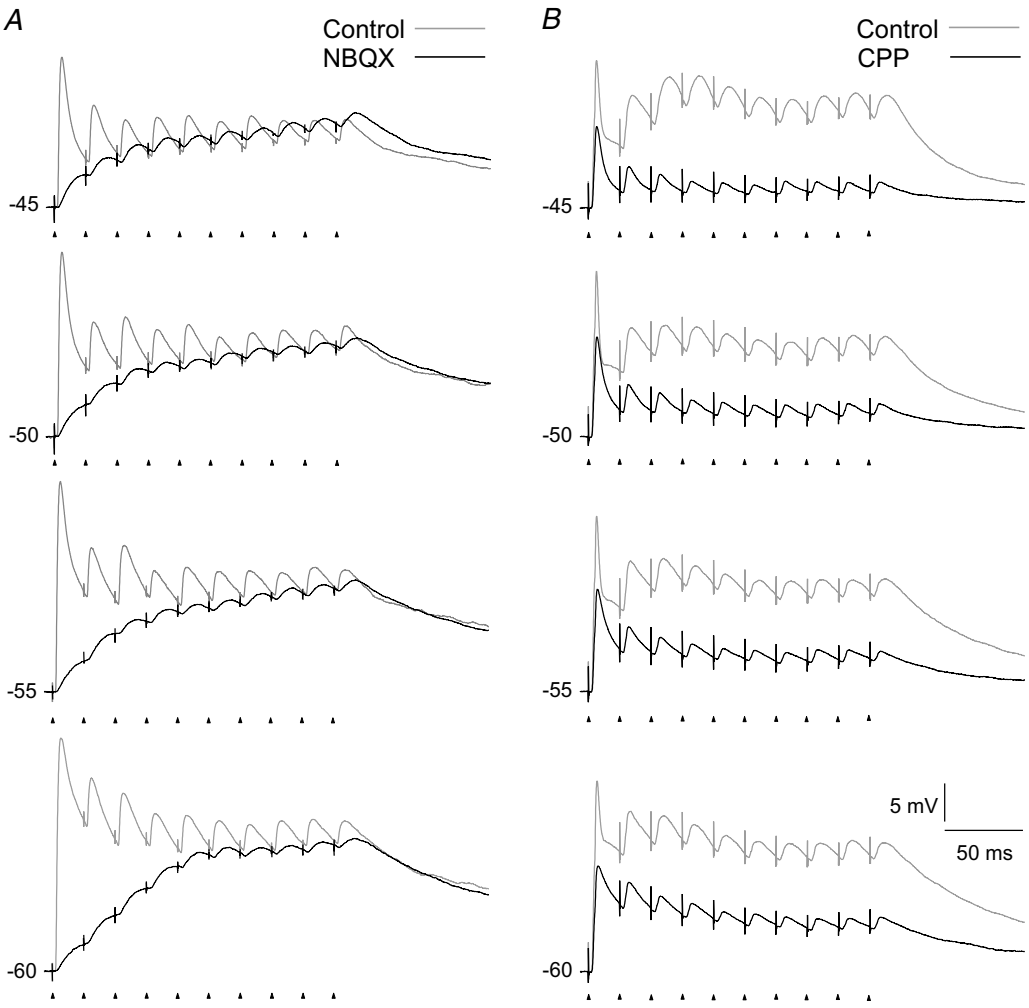

Figure 3. Temporal summation of NMDA-R and AMPA-R mediated EPSPs evoked at different holding potentials

Responses to 50 Hz pulse train stimulation of retinal afferents. *A*, temporal summation of NMDA-R mediated EPSPs. Traces in grey, responses in the control condition before blockade of AMPA-Rs. Traces in black, responses after blockade of AMPA-Rs with 10 μM NBQX. *B*, temporal summation of AMPA-R mediated EPSPs. Traces in grey, responses in the control condition before blockade of NMDA-Rs. Traces in black, responses after blockade of NMDA-Rs with 10 μM CPP. Voltage dependent sodium spikes were blocked by QX222 added to the intracellular solution. Each trace is the average of five repetitive train stimulations. Data in *A* and *B* are from two different cells.

the first pulse of the train in the control condition by application 0.5 mM Ni^{2+} (data not shown).

The finding that the increase of depolarization at the beginning of the response became faster at more depolarized holding potentials could be an effect of the non-linear voltage dependence of the NMDA-R. We therefore recorded NMDA-R mediated EPSPs to single stimulus pulses ($n = 11$). An example of traces from one neuron at the different holding potentials is shown in Fig. 5*A*. It shows that the rise time of the EPSP became faster with the more depolarized holding potentials. This corresponds to the increasing steepness of the initial response to the pulse trains, as described above. Moreover, the amplitude of the EPSPs increased as the holding potential was shifted to more depolarized levels despite the reduced driving potentials. This is consistent with the negative voltage dependence of the NMDA-R in this range of membrane potentials (Mayer *et al.* 1984; Nowak *et al.* 1984). The rise time determined from a single exponential fitted to the rising slope of the EPSPs, decreased from an average of 8.1 ± 0.5 ms at -60 mV to 4.9 ± 0.3 ms at -45 mV holding potential ($P < 0.0001$, d.f. $= 3$; $n = 11$).

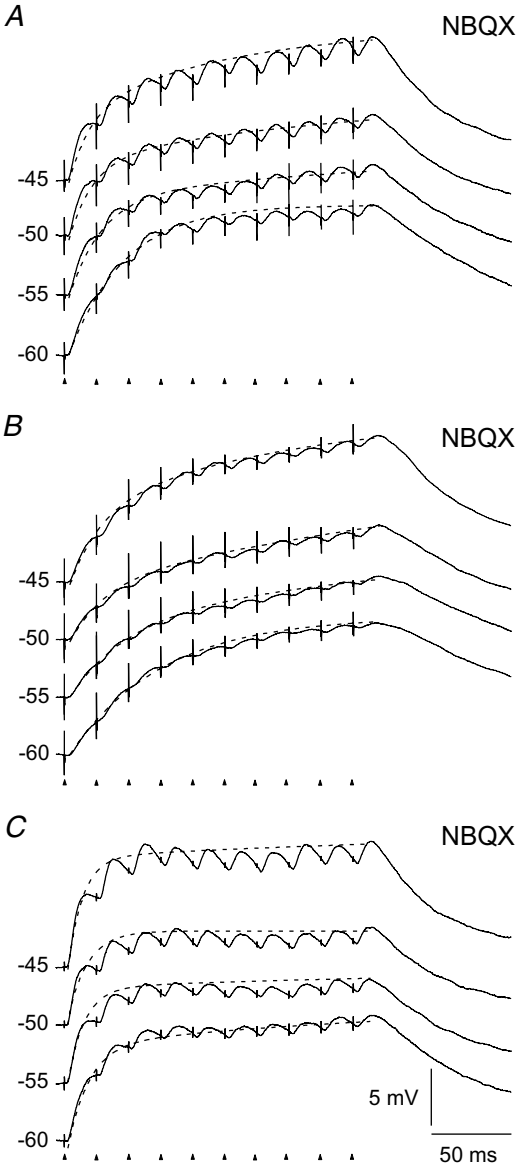

Figure 4. Variation between neurons in rise time and degree of accumulated depolarization during temporal summation of NMDA-R mediated EPSPs
Responses to pulse train stimulation (50 Hz) of retinal afferents. *A–C*, results from three different neurons showing temporal summation of EPSPs mediated by NMDA-Rs. AMPA-Rs were blocked by 10 μM NBQX. The traces are averages of 5 stimulus repetitions. Dashed curves are double exponentials fitted to the peak EPSP after each stimulus pulse.

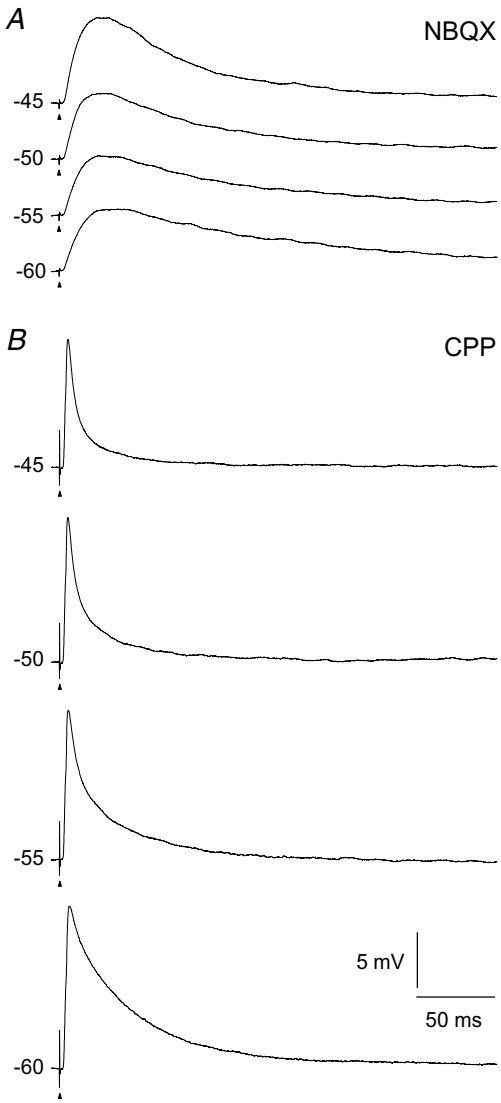

Figure 5. Single-pulse EPSPs evoked at different holding potentials
A, NMDA-R mediated EPSPs. AMPA-Rs were blocked by 10 μM NBQX. *B*, AMPA-R mediated EPSPs. NMDA-Rs were blocked by 15 μM CPP. Each trace is an average of 5 responses. The data in *A* and *B* are from two different cells.

The amplitude of the EPSPs increased from an average of 5.3 ± 0.5 mV at -60 mV to 5.7 ± 0.6 mV at -45 mV holding potential ($P < 0.008$, d.f. $= 3$; $n = 11$).

The traces for the AMPA component of the responses to the pulse trains could be well fitted by single exponential functions which characterized the decay of the EPSPs. Results from a representative neuron are shown in Fig. 6. There was a reduction of the time constant with changes to more depolarized holding potential, on average from 28.3 ± 6.7 ms at -60 mV to 15.3 ± 2.9 ms at -45 mV, but the reduction was not statistically significant ($P = 0.086$, d.f. $= 3$; $n = 7$). The EPSP to a single stimulus pulse decreased in amplitude as the holding potential was changed to more depolarized levels consistent with the linear voltage dependence of these receptors, as illustrated by results from a representative neuron in Fig. 5*B*. The amplitude of the EPSPs decreased from an average of 11.6 ± 1.8 mV at -60 mV to 9.1 ± 1.2 mV at -45 mV holding potential ($P < 0.004$, d.f. $= 3$, $n = 7$).

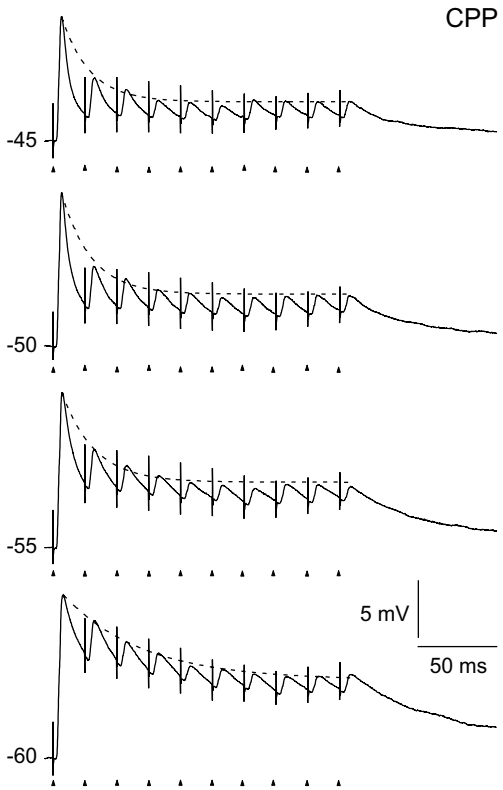

Figure 6. Temporal summation of AMPA-R mediated EPSPs at different holding potentials evoked by stimulation of retinal afferents

Responses to 50 Hz pulse train stimulation during blockade of NMDA-Rs with 15 μM CPP. Averages of 5 repetitions of stimulation. Dashed lines, single exponential functions fitted to EPSP peaks.

Temporal summation of EPSPs at different stimulus frequencies

As illustrated in Figs 3*A* and 4, the increasing depolarization of the NMDA component during stimulus trains at 50 Hz was due to the long duration of the single EPSPs compared with the interpulse intervals. This suggests that the build-up of depolarization should be even stronger at shorter interpulse intervals. However, the synaptic depression of the NMDA-Rs increases with shortening of interpulse intervals, as well (Chen *et al.* 2002; Kielland & Heggelund, 2002) and this could counteract a stronger build-up of depolarization at higher stimulus frequencies.

Recordings of temporal summation of NMDA-R mediated EPSPs at different frequencies in the range of 50–100 Hz demonstrated a substantial increase of depolarization with increasing stimulation frequency. This is shown for a representative neuron in Fig. 7*A*. The neuron was stimulated with trains at three different frequencies (50, 80 and 100 Hz) at a holding potential of -50 mV. Comparison of the depolarization developed by the NMDA component (black traces), and the combined contribution of this and the AMPA component (grey traces), shows that the NMDA component elicited the major depolarization at all frequencies. Moreover, the dominance of the NMDA component increased considerably with the increasing pulse frequency. Only at the beginning of the train, and in particular at the first pulse, did the AMPA component have a strong, dominant contribution. The average change in membrane potential generated by the NMDA component during the pulse train increased from 8.7 ± 0.8 mV at 50 Hz to 14.5 ± 1.7 mV at 100 Hz train stimulation ($P < 0.003$, d.f. $= 2$; $n = 6$) demonstrating that the summation of the EPSPs gave stronger depolarization at higher stimulus frequency despite the synaptic depression.

Effects of different stimulation frequencies on the summation properties of the AMPA component are illustrated by results from a representative neuron in Fig. 7*B*. The same three stimulation frequencies and the same holding potentials (-50 mV) were used as for the neuron in Fig. 7*A*. The results showed that the depolarization decreased more rapidly during the train with increasing stimulus frequency. The time constant of single exponentials fitted to the traces decreased from 20.6 ± 2.6 ms at 50 Hz, to 11.6 ± 1.4 ms at 100 Hz train ($P < 0.041$, d.f. $= 2$, $n = 5$). This is consistent with the fast characteristics of synaptic depression of the AMPA-R mediated input (Chen *et al.* 2002; Kielland & Heggelund, 2002). However, the degree of increased depolarization above the holding potential at the end of the train was about the same at all three stimulus frequencies (3.5 ± 0.4 mV; $P < 0.25$, d.f. $= 2$; $n = 5$). This may explain why the drop of the AMPA component was less than the

gain of the NMDA component such that the combined depolarization of the both components increased with the increasing stimulus frequency (Fig. 7, grey traces).

Synaptic depression of the AMPA and NMDA components can be seen by comparing the size of the successive EPSPs in the traces in Figs 3, 4, 6 and 7 Quantitatively it was difficult to measure the magnitude of the depression for the NMDA component, because the amplitude of most EPSPs were still quite large when the next stimulus pulse was delivered. However, qualitative comparison of the traces for the AMPA and the NMDA components shows that the depression was stronger for the AMPA than for the NMDA component consistent with the fast desensitization of the AMPA-Rs (Chen *et al.* 2002; Kielland & Heggelund, 2002).

Firing pattern at different holding potentials

The temporal summation properties of the EPSPs of the AMPA and NMDA components, presented above, could explain the contributions of the two components to the firing patterns at the different holding potentials.

The typical firing pattern generated by the isolated NMDA component is illustrated by the traces in Fig. 8*A*. At −60 mV, the EPSPs showed the characteristic summation pattern for this component, but no spikes were elicited. As the holding potential was stepped up to more depolarized levels, spiking occurred first in the later parts of the train, and then also in the earlier parts. At the most depolarized holding potential (−45 mV), the neuron fired spikes throughout the whole train. Thus, spike generation of the NMDA component is not limited to the later parts

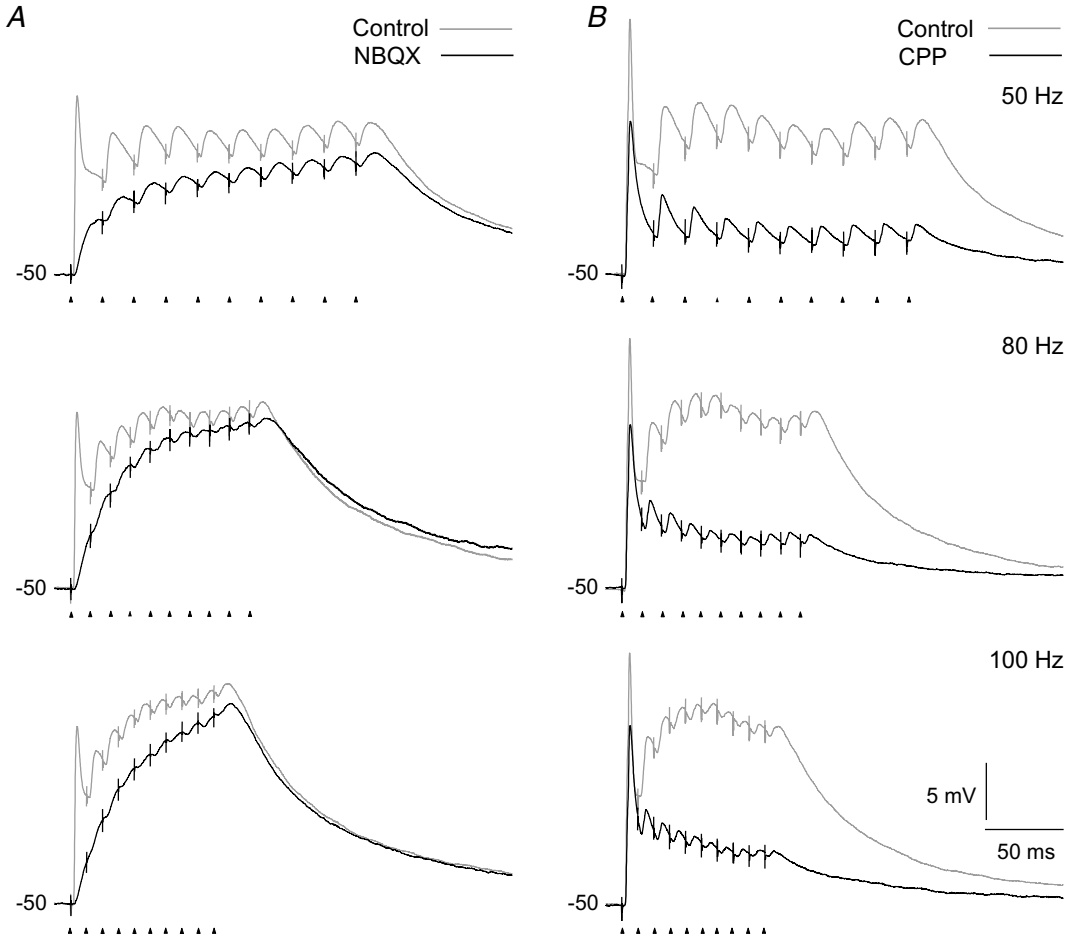

Figure 7. Temporal summation of evoked EPSPs at different pulse train frequencies
Responses to three different frequencies of pulse train stimulation at a holding potential of −50 mV. *A*, results for the NMDA component. Grey traces, responses in the control condition before wash-in of AMPA-R antagonist. Black traces, responses after application of 10 μM NBQX. *B*, results for the AMPA component. Grey traces, responses in control condition before wash-in of NMDA-R antagonist. Black traces, responses after application of 15 μM CPP. Data in *A* and *B* are from two different cells. Each trace is an average of 5 responses.

of a pulse train, but may occur even to the first pulse at sufficiently depolarized holding potentials. This was seen in all cells tested ($n = 6$). Clearly, the effect of the NMDA component on sustained spike firing will be highly sensitive to inputs from the brainstem or cortex that modulate the membrane potential of the neuron.

To study the contribution of the AMPA component, we blocked ($n = 7$) the NMDA-Rs with CPP. The effect of the isolated AMPA component on the firing pattern is illustrated by the traces in Fig. 8*B*. At all holding potentials the blockade of the NMDA component had no effect on spiking to the first 1–2 pulses, but all spikes to the subsequent pulses of the train were abolished, consistent with the pronounced amplitude reduction of the EPSPs during the train described for the AMPA component in the previous section. This demonstrates

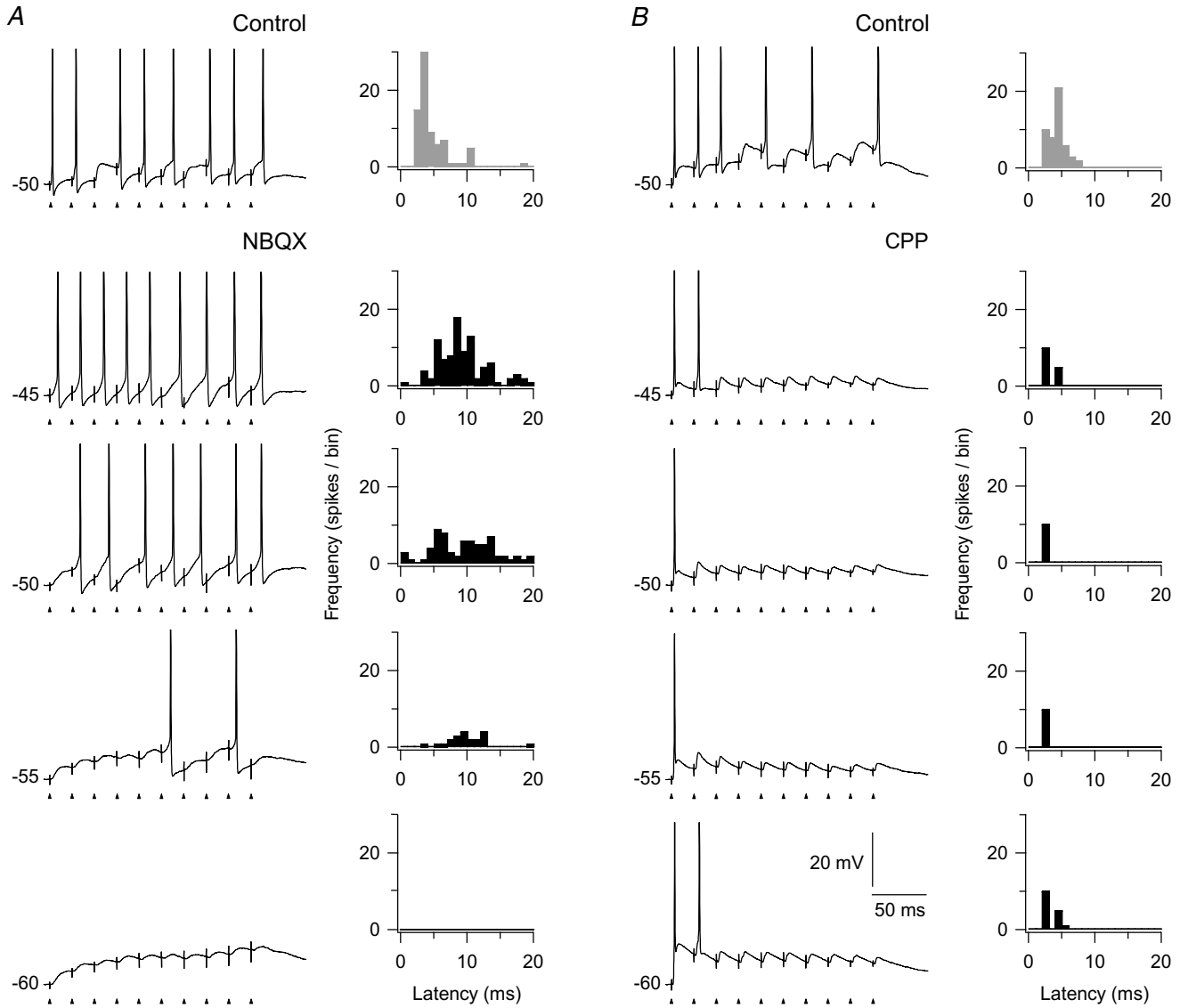

Figure 8. Spike-firing pattern and spike timing to train stimulation of retinal afferents at different holding potentials

Each trace is from single train stimulation at 50 Hz. *A*, left, results for the NMDA component. Upper trace, response in the control condition before application of the AMPA-R antagonist. The other traces were recorded after blockade of AMPA-Rs with 10 μM NBQX. Right, histograms showing the distribution of latencies of the spikes, in the respective conditions, calculated from the closest preceding pulse in the train stimulus. Each histogram is based on spikes from 10 repetitions of the train stimulation. Bin width, 1 ms. The uppermost histogram (with grey bars) is for the control condition. *B*, left, results for the AMPA component. Uppermost trace, for the control condition before application of antagonist. The other traces, after wash-in of 15 μM CPP. Right, histograms of spike latencies for spikes from 10 train stimulations, as in *A*.

that the NMDA component was necessary for generation of action potentials after the first few pulses in the train stimulus.

To study the precision of spike timing with respect to timing of pulses in the train stimuli, we determined the latency of a spike from the nearest preceding pulse. Results for the NMDA and the AMPA component are presented in the histograms in Fig. 8*A* and *B*, respectively. Each histogram is based on the response to 10 stimulus presentations. The histograms in Fig. 8*A* present results for the isolated NMDA component. The results demonstrate that the blockade of AMPA-Rs eliminated the precisely timed spikes, and that the latencies of the elicited spikes were widely scattered. In the control condition at −50 mV (Fig. 8*A*, upper histogram with grey bars) the mean latency of the spikes was 4.2 ± 0.2 ms, and the coefficient of variation was 0.29. The latency at the same membrane potential for the isolated NMDA component had a mean of 9.8 ± 0.6 ms, and a variation coefficient of 0.49. There was no apparent change in the variability related to the holding potential. At −45 mV about the same mean latency (9.4 ms ± 0.4) and variation coefficient (0.41) was found despite the fact that at −45 mV the number of spikes was about the same as number of stimulus pulses. Similar results were obtained for all neurons tested with pulse trains at 50 Hz ($n = 4$). Tests with pulse trains of higher frequencies (80 and 100 Hz) also showed similar wide scatter of spike latencies as shown by the histograms in Fig. 9*A* and *B*. The results demonstrate that the single EPSPs mediated by the NMDA component did not trigger a precisely timed spike. Rather the level of depolarization built up by the temporal summation of this component generated a firing pattern in many respects similar to what is seen by a current step. This is illustrated in Fig. 9 where the firing patterns to an 80 Hz and a 100 Hz pulse train are compared to the firing pattern elicited by current steps through the recording electrodes. The response patterns to the train stimuli and to the current steps were characterized by the long latency from the start of the stimulus to the first spike, and a slightly accelerating firing rate.

The histograms in Fig. 8*B* show that the spikes elicited by the isolated AMPA component occurred with short latency from the preceding stimulus pulse and that there was little variation of this latency between spikes. At a holding potential of −50 mV the mean latency was 2.6 ± 0.01 ms, and the coefficient of variation was 0.02. Similar values were found at the other holding potentials, and for all neurons tested ($n = 5$). The latency of the spike to the second pulse in the train was slightly longer than the latency of the first pulse, presumably due to after-hyperpolarization following the first spike. In the control condition at −50 mV (Fig. 8*B*) the mean latency was 4.3 ± 0.2 ms, and the coefficient of variation 0.3.

Role of the AMPA component in preserving precise spike timing at the synaptic relay

The role of the AMPA component in determining precise timing of spikes during the pulse train was not restricted to the spikes elicited by the first few stimulus pulses. This appears from the histograms in Fig. 8*A* by comparison of the distributions of spike latencies for the isolated NMDA component (histograms with black bars), with the distributions in the control condition when both AMPA and NMDA components were present (histogram with grey bars). The number of poorly timed spikes was considerably lower in the control condition than in the condition in which the AMPA-Rs were blocked. Accordingly, the AMPA component contributed to precise timing of the spikes even during the later part of the train, although the isolated AMPA component then was insufficient for spike generation. This is consistent with the interpretation that the NMDA component provides current that counteracts the rapid depression of the AMPA-Rs and keeps the neuron depolarized at a level closer to the threshold for action potential generation. When this level is high enough, the relatively weak but precisely timed EPSP of the AMPA component may be sufficient to trigger a spike, and thereby determine the precise timing of the spike.

Effects of frequency changes in the stimulus train

In the results presented above the stimulus trains were delivered without immediately preceding synaptic input. However, *in vivo* there is continuous synaptic input to TC neurons due to maintained activity in the retinal ganglion cells, and this presumably induces a sustained synaptic depression at the retinogeniculate synapses. Thus, when there is a sudden increase in the retinal input to a TC neuron *in vivo,* caused by for instance a visual stimulus flashed on its receptive field, the response is weakened by a sustained synaptic depression not present in our conditions with sudden onset of input. To study effects of preceding input activity on the response to pulse trains used in the experiments presented in the previous sections, we used ($n = 10$) a three-part stimulus train, the first part with 20 Hz pulses (typical frequency of maintained activity of retinal ganglion cells *in vivo*; Balkema & Pinto, 1982; Stone & Pinto, 1992), the second part with 50 Hz pulses, and the final part with 20 Hz pulses. The final part was introduced to observe after-effects of the 50 Hz train.

Effects of the immediately preceding input activity on the summation of EPSPs at different holding potentials are illustrated by results from two neurons in Fig. 10. Responses to the three-part stimulus train are shown by the black traces; the grey traces show control responses when only the 50 Hz train was given. Figure 10*A* shows results from a neuron for which the NMDA component

was studied. The most pronounced effect of the preceding 20 Hz stimulation was the quite pronounced depolarization of the membrane potential during this first part of the three-part stimulus. However, we found no marked effects of the preceding stimulus pulses on the response to the 50 Hz train apart from a slightly increased depolarization to the first stimulus pulse. The response to the final 20 Hz pulses demonstrated a rather slow decay of the effects after the 50 Hz train. Figure 10*B* shows results from a neuron for which the AMPA component

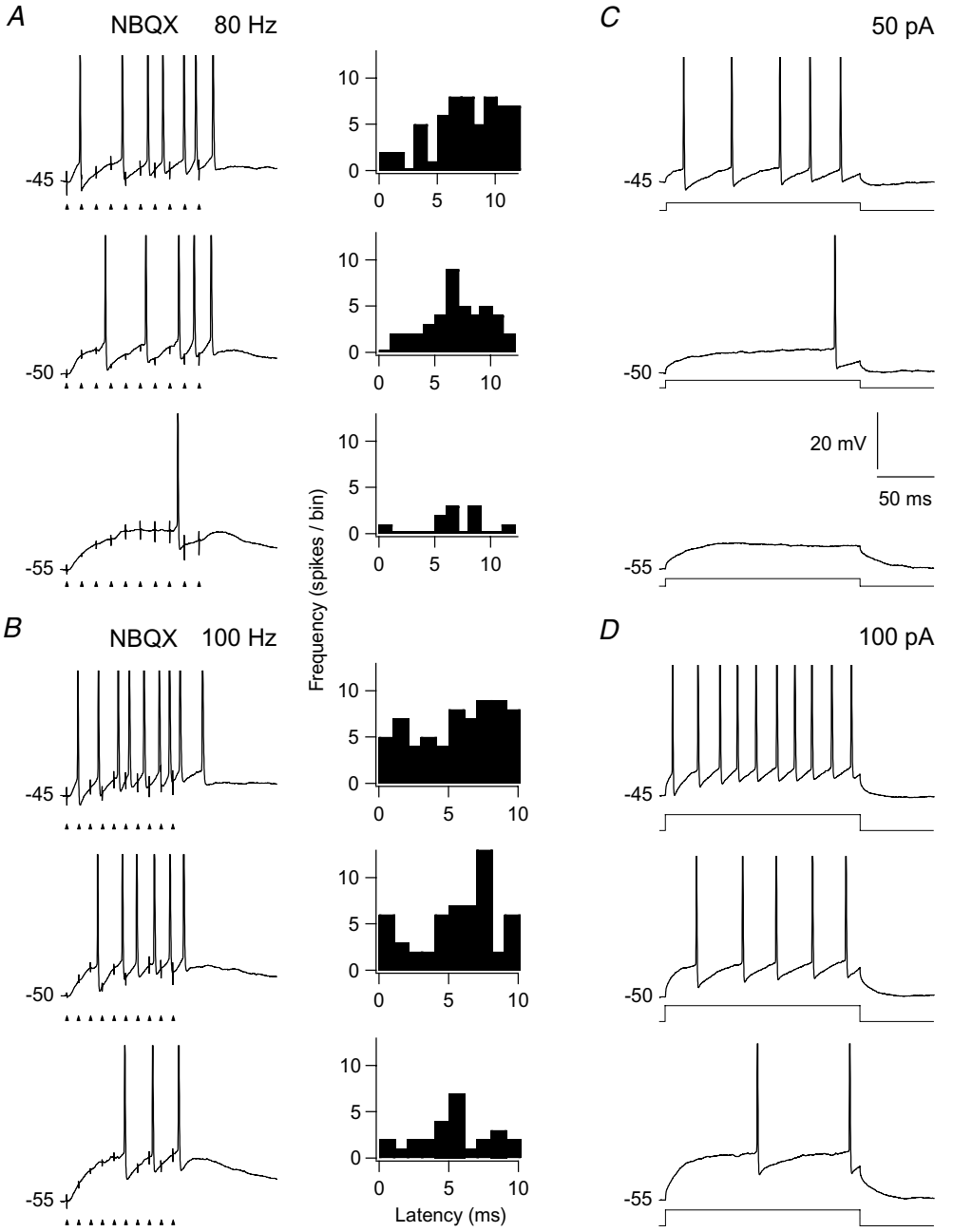

Figure 9. Similarities between NMDA-R mediated responses to pulse-train stimulation and responses to a current step
A, left, firing pattern evoked at three different holding potentials by pulse train stimulation of retinal afferents at 80 Hz during application of 10 μM NBQX. Right, corresponding distribution of spike latencies, as in Fig. 8. *B*, similar results as in *A* except for train stimulation at 100 Hz. *C*, firing pattern evoked by a depolarizing current step (50 pA) delivered at the same three holding potentials as in *A*. *D*, firing pattern evoked by a depolarizing current step (100 pA) at the same three holding potentials as in *A*.

was studied. For this component the preceding 20 Hz stimulation induced a pronounced depression of the EPSP amplitudes at the beginning of the 50 Hz train, as predicted, and a fast decay of the effects after the 50 Hz train.

Effects of preceding 20 Hz stimulation on the spike firing pattern elicited by the 50 Hz pulse train are illustrated in Fig. 11. Figure 11*A* shows results from a neuron for which the firing elicited by the isolated NMDA component was studied. The figure shows that for this component, the

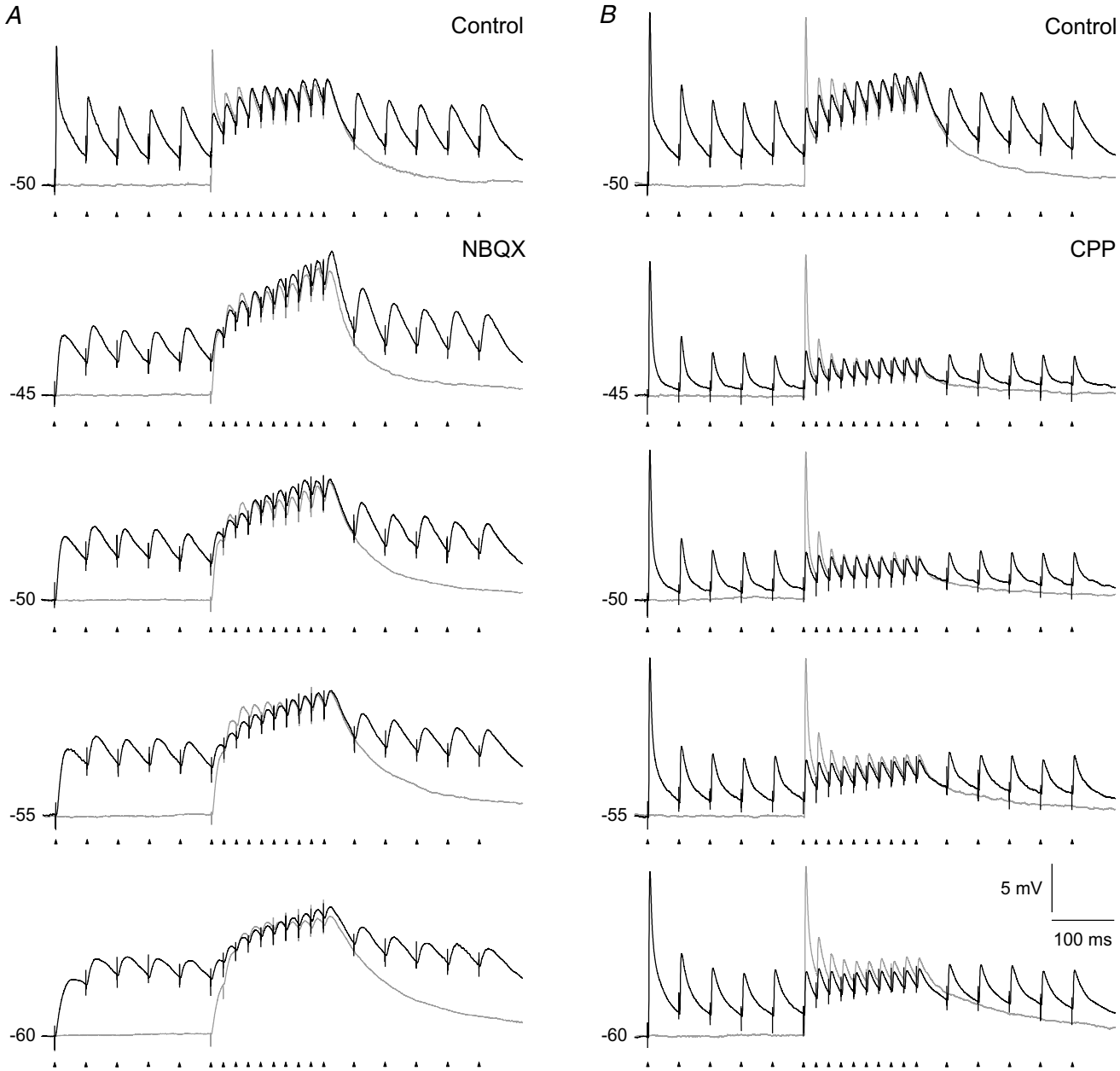

Figure 10. Influence of immediately preceding synaptic input on the EPSP amplitudes evoked by pulse train stimulation at different holding potentials

Comparison of responses to two different patterns of pulse train stimulation of retinal afferents. Black traces, responses to a three-part stimulus train with the first part consisting of 5 pulses at 20 Hz, the second part with 10 pulses at 50 Hz, and the third part with 5 pulses at 20 Hz. Grey traces, control recordings of responses to the 50 Hz train stimulus alone. *A*, responses of the NMDA component. Top panel, control before wash-in of AMPA-R antagonist. Lower panels, traces at different membrane potentials after blockade of AMPA-Rs with 10 μM NBQX. *B*, responses of the AMPA component. Top panel, control before wash-in of NMDA-R antagonist. Lower panels, traces after blockade of NMDA-Rs with 15 μM CPP. Each trace is an average of 5 responses. The data in *A* and *B* are from two different cells.

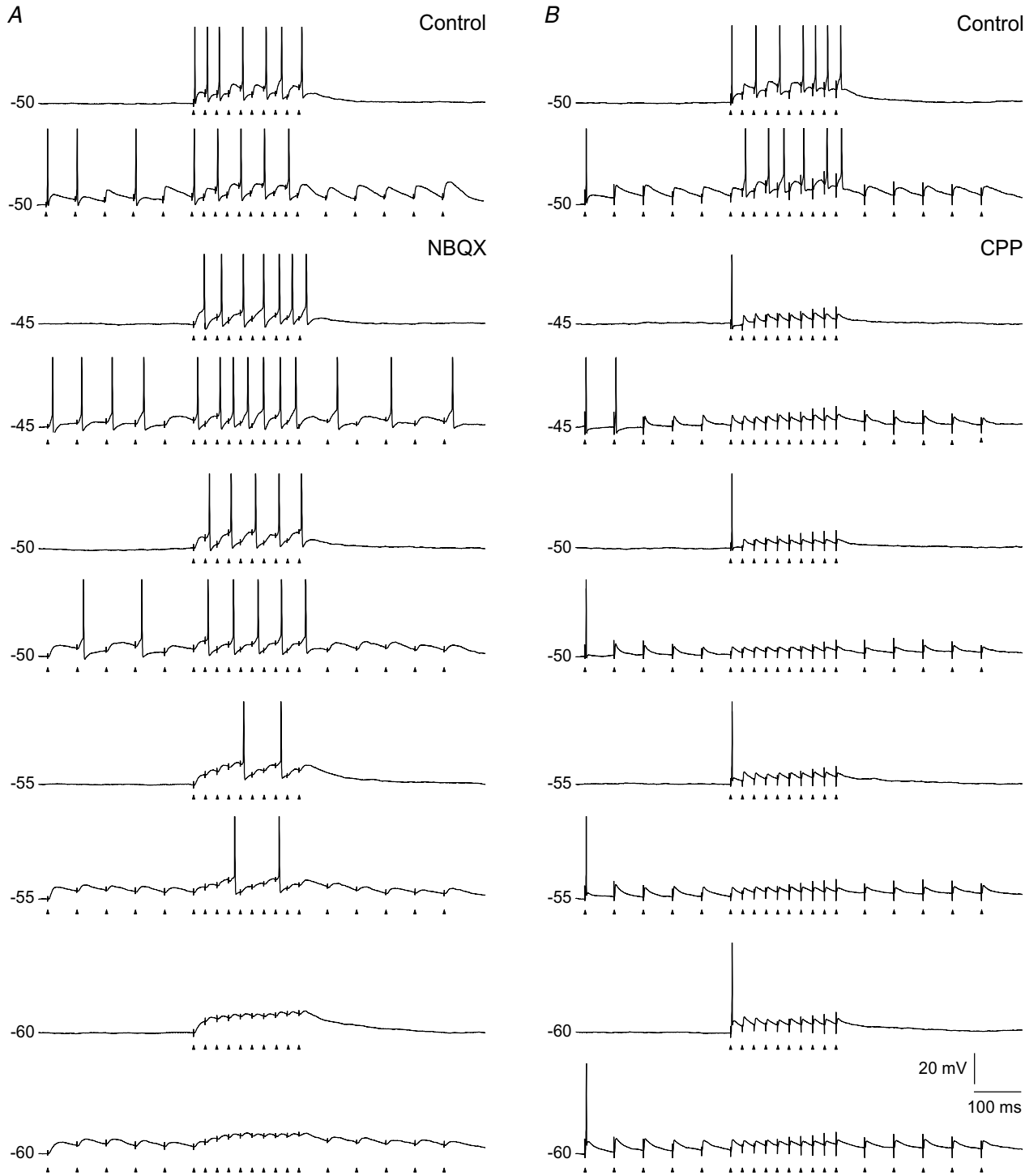

Figure 11. Influence of immediately preceding synaptic input on spike patterns evoked by pulse train stimulation at different holding potentials

Comparison of responses to the same two patterns of pulse train stimulation of retinal afferents as in Fig. 10. For each holding potential there is a pair of traces; the upper trace is response to the 50 Hz train in the control condition without preceding synaptic input; the lower trace is response in the condition with 5 pulses at 20 Hz preceding and following the 50 Hz train. *A*, responses of the NMDA component. Top pair of panels, control before wash-in of AMPA-R antagonist. Lower pairs of panels, traces at different membrane potentials after blockade of AMPA-Rs with 10 μM NBQX. *B*, responses for the AMPA component. Top pair of panels, control before wash-in of NMDA-R antagonist. Lower pairs of panels, traces after blockade of NMDA-Rs with 15 μM CPP. The data in *A* and *B* are from two different cells.

preceding 20 Hz stimulation had no marked effects on the firing pattern to the 50 Hz train, except for a slight reduction in the latency to the first spike. However, for the AMPA component, as shown in Fig. 11*B* by results from another neuron, the preceding 20 Hz stimulation generated a sufficiently strong depression to prevent spike generation at the beginning of the 50 Hz train at all holding potentials. These results suggest that the amplitude of the AMPA-R mediated EPSPs *in vivo,* at such a firing rate, is too small to generate action potentials due to sustained depression of the receptors, and that summation with the NMDA component is typically necessary for spike generation even initially after an abrupt increase in the frequency of the retinal input.

Discussion

The results demonstrate a differential role of the NMDA and the AMPA components in the synaptic transfer of retinal input to TC neurons. The NMDA component gave increasing depolarization through temporal summation of EPSPs during train stimulation, despite synaptic depression. This build-up of depolarization was due to the long duration of the NMDA component of the single EPSPs, and to effects of the non-linear voltage dependence on rise-time and amplitude of the EPSPs during the increasing depolarization. The depolarization could provide sustained firing of the neuron with a firing rate that depended on the holding potential. This is a mechanism for sustained firing that is very sensitive to modulatory inputs that regulate the membrane potential of the neuron. The isolated AMPA component was rather ineffective for spike generation. In the conditions where the pulse train was delivered without preceding synaptic activity, the AMPA component could generate short-latency spikes at the beginning of the train, but when the same pulse train was preceded by a few pulses in the frequency range of maintained activity of retinal ganglion cells, these initial spikes were abolished due to synaptic depression. However, added to the NMDA component the AMPA component contributed significantly to spike generation, and was necessary for the precise timing of the spikes throughout the response.

TC neurons in LGN are normally influenced by many factors besides the glutamatergic input from retina that we studied, and one might ask to what extent our results apply to a more realistic *in vivo* situation. Other inputs modulate the activity pattern of the neurons in a state-dependent manner and change the firing pattern through GABAergic inputs. However, many of these influences, like most inputs from the brainstem, operate on a coarse time scale and exert their effects on various intrinsic conductances that induce relatively slow adjustments of the membrane potential (McCormick, 1992). The glutamatergic input from cortex seems, at least partly, to have similar effects. A single stimulus pulse to cortical afferents evokes just a minor EPSP in the TC neuron, but a train of pulses elicits EPSPs that summate to a more sustained depolarization (Lindström & Wróbel, 1990; Turner & Salt, 1998; von Krosigk *et al.* 1999). Intrinsic interneurons and neurons in the thalamic reticular nucleus, on the other hand, can sculpt the activity of TC neurons through fast $GABA_A$ inhibition. The interneurons generate a fast IPSP that follows the EPSP elicited by a spike in the retinal afferents (Lindström, 1982; Crunelli *et al.* 1987). This might slow down the build-up of depolarization through the NMDA component, but the degree of such slowdown could be rather limited since the duration of these IPSPs is considerably shorter than the duration of the NMDA-R mediated EPSPs. However, the interneurons and neurons in the thalamic reticular nucleus can provide inhibition also through $GABA_B$ receptors (Roy *et al.* 1984; Crunelli *et al.* 1988), and this could stop sustained firing and possibly induce burst firing in TC neurons by sufficiently long-lasting hyperpolarization (McCormick & Pape, 1990).

Responses of non-lagged TC neurons to an optimal visual stimulus flashed on the receptive field vary from predominantly transient to highly sustained. The transient/sustained behaviour is related to sleep states varying across non-REM sleep to drowsy or awake states (Coenen & Vendrik, 1972), and to changes in the EEG power spectrum from low frequency dominance to high frequency dominance (Funke & Eysel, 1992, 2000; Li *et al.* 1999). Several *in vivo* studies suggest that the sustained response is generated by the NMDA component of the sensory input (Salt, 1987; Hartveit & Heggelund, 1990; Heggelund & Hartveit, 1990; Funke *et al.* 1991; Zhang & Kelly, 2001), and the results from the present study suggest that the change to more sustained firing is caused by mechanisms that depolarize the neuron and bring the NMDA component of the retinal input toward the threshold for spike generation. Such changes in membrane potential might be elicited by several state-related mechanisms. The best characterized one is increased input from cholinergic and other activation related brainstem nuclei (Francesconi *et al.* 1988; Funke & Eysel, 1992; Humphrey & Saul, 1992; Funke *et al.* 1993; Hartveit & Heggelund, 1992, 1993, 1995; Hartveit *et al.* 1993; Fjeld *et al.* 2002) that depolarize TC neurons (Curró Dossi *et al.* 1991; Timofeev *et al.* 1996) by reducing the potassium current I_{leak} (McCormick & Pape, 1990; McCormick, 1992), in addition to other possible effects that might affect the amplitudes and temporal summation of EPSPs like membrane resistance and voltage-dependent conductances. The sustained depolarization of TC neurons generated by a pulse train in cortical afferents (Lindström & Wróbel, 1990; Turner & Salt, 1998; von Krosigk *et al.* 1999) may be an even more powerful mechanism

for regulation of spike firing generated by the NMDA component.

State-dependent changes of response in TC neurons in LGN are usually related to a burst and a tonic mode, which are most clearly defined *in vitro* (Jahnsen & Llinas, 1984*a*,*b*; McCormick & Pape, 1990; McCormick, 1992). Burst mode occurs at membrane potentials hyperpolarized below about −60 mV and is characterized by rhythmic generation of low-threshold calcium bursts. Tonic mode occurs at depolarized membrane potentials above about −60 mV and is characterized by firing of single spikes. However, it is not clear how these two modes relate to responses of TC neurons to visual stimuli *in vivo*, and in particular, how they relate to the state-dependent changes from a mainly transient to a more sustained response to a visual spot stimulus. First, the *in vivo* studies were typically done by extracellular recording. Thus, the actual membrane potential of the neurons is unknown. Second, the transient-sustained changes are continuous (Funke & Eysel, 1992, 2000; Li *et al.* 1999) rather than being a shift between two discrete modes. Third, the visual response of TC neurons is basically similar to that of the retinal input and not considerably different as it would be if generated primarily by calcium bursts (Mastronarde, 1987*a*; Hartveit *et al.* 1993; Hartveit & Heggelund, 1995; Usrey *et al.* 1997; Fjeld *et al.* 2002). The response in TC neurons may be considerably weaker than the retinal input, particularly with respect to the sustained response component. The initial transient is generated in retina and is typically rather faithfully transferred to the LGN neuron (Hartveit *et al.* 1993; Hartveit & Heggelund, 1995; Fjeld *et al.* 2002). Following this transient there is typically at least some additional firing that is mainly single spike firing (e.g. Hubel & Wiesel, 1961; Coenen & Venderik, 1972). Even in conditions where the EEG power spectrum is dominated by low frequencies, there is some sustained firing (Coenen & Venderik, 1972; Livingstone & Hubel, 1981; Funke & Eysel, 2000), and this typically consists of single spikes rather than spike bursts (Coenen & Venderik, 1972; Livingstone & Hubel, 1981). Thus, the firing of TC neurons during optimal visual stimulation seems typically to occur in tonic mode. Possibly, the initial high-frequency transient response of the retinal input is sufficient to switch the neuron from a possible burst mode to the tonic mode. The changes we observed in the response to the train stimulation with variation of the holding potential, from just a few spikes at the beginning of the train to a more sustained firing throughout the train, occurred in a tonic mode. We suggest that the increasing sustained firing at more depolarized holding potentials, which shifted the NMDA component toward spike firing threshold, is related to *in vivo* changes along the transient–sustained axis. This mechanism could play a key role in regulation of the impact of sensory input to cortex during different degrees of arousal, attention, and vigilance, and is a mechanism that can be controlled from both the brainstem and cortex.

Blitz & Regehr (2003) found that spikes at the beginning of a train stimulus are elicited by the AMPA component, whereas spikes in the later parts of the train are elicited by the NMDA component. Corresponding results have been found in other sensory nuclei (Salt, 1987; Zhang & Kelly, 2001). Other results have demonstrated that also early spike firing can be mediated by the NMDA component (Sanchez *et al.* 2007). The results of Blitz & Regehr (2003) were obtained at a holding potential of −55 mV. As shown by Fig. 8, we got similar results at this membrane potential. However, at more depolarized membrane potential, the NMDA component could elicit spikes throughout the pulse train, even to the first pulse in the train (Fig. 8*A*, −45 mV). This suggests that the apparent discrepancy between the previous studies could at least partly be due to a difference of membrane potential at which the firing pattern was studied. Moreover, we found strong stimulus induced depolarization mediated by the NMDA-Rs throughout the pulse train; even at the first pulse of the train. Thus, also at membrane potentials at which the NMDA component alone was insufficient to elicit early spikes, this component contributed with a substantial depolarization that together with the AMPA component could reach firing threshold.

The contribution of the NMDA component to retinogeniculate transmission *in vivo* is most likely even more pronounced than indicated by our data from responses to the pulse trains presented without immediately preceding synaptic input. Our data with the three-part stimulus train (Figs 10 and 11) demonstrated that stimulation with pulses in the frequency range of normal maintained firing of retinal ganglion cells *in vivo* immediately before a 50 Hz pulse train depressed the AMPA component to such extent that it failed to elicit spikes at all. This suggests that summation of AMPA-R and NMDA-R mediated EPSPs is necessary for spike generation even at the start of a sudden increase of retinal input, as presumably occurs at the onset of a visual stimulus. Moreover, the results from these experiments suggest that temporal summation of NMDA-R mediated EPSPs elicited by the maintained activity of retinal ganglion cells may generate a considerable depolarization of TC neurons that can contribute to keeping the neuron in a tonic mode.

Our results demonstrate that the latency of spikes elicited by the NMDA component was longer than the latency in the condition with both NMDA and AMPA components present, even in the condition when the NMDA component alone elicited a number of action potential equal to the number of pulses in the stimulus train (see histogram in Fig. 8 for −45 mV holding potential). This is consistent with the finding of Sanchez *et al.* (2007) for auditory responses in the inferior colliculus that the NMDA component is more important for spike generation in long-latency neurons than in short-latency neurons.

The lack of precise spike timing of the NMDA component combined with the precise spike timing of the AMPA component (Blitz & Regehr, 2003) does occasionally lead to a more irregular firing pattern including spike doublets (see the upper two traces in Fig. 1). In extracellular recordings such instances might be falsely regarded as burst related. However, the main result from our study concerning the combined effect of the AMPA and NMDA components on spike generation was a substantially increased fidelity of spike timing of the afferent input compared to the spike timing of the isolated NMDA component. This suggests that precise preservation of spike timing at the retinogeniculate relay (Mastronarde, 1987*b*; Reinagel & Reid, 2000, 2002) is due to an interplay between the AMPA and the NMDA components in which the NMDA component depolarizes the TC neuron toward the threshold for spike generation, and on top of that the typically small AMPA component may generate a precisely timed spikes. High preservation of timing at the retinogeniculate relay during visual stimulation *in vivo* was demonstrated by high cross-correlation of spike timing in pairs of non-lagged TC neurons and a connected retinal ganglion cell (Mastronarde, 1987*b*) suggesting that action potentials throughout the visual response are transmitted with preservation of precise timing. In lagged cells on the other hand, which have their functional input mediated through NMDA receptors (Heggelund & Hartveit, 1990), the cross-correlation was considerably lower (Mastronarde, 1987*b*). The preservation of precise spike timing may be essential for certain types of synaptic plasticity at the cortical level that is spike timing dependent (Schuett *et al.* 2001; Jacob *et al.* 2007).

References

Balkema GW & Pinto LH (1982). Electrophysiology of retinal ganglion cells in the mouse: a study of a normally pigmented mouse and a congenic hypopigmentation mutant, pearl. *J Neurophysiol* **48**, 968–980.

Blitz DM & Regehr WG (2003). Retinogeniculate synaptic properties controlling spike number and timing in relay neurons. *J Neurophysiol* **90**, 2438–2450.

Blitz DM & Regehr WG (2005). Timing and specificity of feed-forward inhibition within the LGN. *Neuron* **45**, 917–928.

Chen CF, Blitz DM & Regehr WG (2002). Contributions of receptor desensitization and saturation to plasticity at the retinogeniculate synapse. *Neuron* **33**, 779–788.

Coenen AML & Vendrik AJH (1972). Determination of the transfer ratio of cat's geniculate neurons through quasi-intracellular recordings and the relation with the level of alertness. *Exp Brain Res* **14**, 227–242.

Crunelli V, Haby M, Jassik-Gerschenfeld D, Leresche N & Pirchio M (1988). Cl^- and K^+-dependent inhibitory postsynaptic potentials evoked by interneurones of the rat lateral geniculate nucleus. *J Physiol* **399**, 153–176.

Crunelli V, Kelly JS, Leresche N & Pirchio M (1987). On the excitatory postsynaptic potential evoked by stimulation of the optic tract in the rat lateral geniculate-nucleus. *J Physiol* **384**, 603–618.

Crunelli V, Lightowler S & Pollard CE (1989). A T-type Ca^{2+} current underlies low-threshold Ca^{2+} potentials in cells of the cat and rat lateral geniculate nucleus. *J Physiol* **413**, 543–561.

Crunelli V, Tóth TI, Cope DW, Blethyn K & Hughes SW (2005). The 'window' T-type calcium current in brain dynamics of different behavioural states. *J Physiol* **562**, 121–129.

Curró Dossi R, Paré D & Steriade M (1991). Short-lasting nicotinic and long-lasting muscarinic depolarizing responses of thalamocortical neurons to stimulation of mesopontine cholinergic nuclei. *J Neurophysiol* **65**, 393–406.

Deschênes M, Paradis M, Roy JP & Steriade M (1984). Electrophysiology of neurons of lateral thalamic nuclei in cat: resting properties and burst discharges. *J Neurophys* **51**, 1196–1219.

Deschênes M, Roy JP & Steriade M (1982). Thalamic bursting mechanism, an inward slow current revealed by membrane hyperpolarization. *Brain Res* **239**, 289–293.

Fjeld IT, Ruksenas O & Heggelund P (2002). Brainstem modulation of visual response properties of single cells in the dorsal lateral geniculate nucleus of cat. *J Physiol* **543**, 541–554.

Francesconi W, Müller CM & Singer W (1988). Cholinergic mechanisms in the reticular control of transmission in the cat lateral geniculate nucleus. *J Neurophysiol* **59**, 1690–1718.

Funke K & Eysel UT (1992). EEG-dependent modulation of response dynamics of cat dLGN relay cells and the contribution of corticogeniculate feedback. *Brain Res* **573**, 217–227.

Funke K & Eysel UT (2000). Quantitative aspects of the state-dependent co-variation of cat lateral geniculate and perigeniculate visual activity. *Neuroreport* **11**, 1031–1037.

Funke K, Eysel UT & Fitzgibbon T (1991). Retinogeniculate transmission by NMDA and non-NMDA receptors in the cat. *Brain Res* **547**, 229–238.

Funke K, Pape H-C & Eysel UT (1993). Noradrenergic modulation of retinogeniculate transmission in the cat. *J Physiol* **463**, 169–191.

Hartveit E & Heggelund P (1990). Neurotransmitter receptors mediating excitatory input to cells in the cat lateral geniculate nucleus. II. Nonlagged cells. *J Neurophysiol* **63**, 1361–1372.

Hartveit E & Heggelund P (1992). Brain-stem influence on visual response of lagged and nonlagged cells in the cat lateral geniculate nucleus. *Vis Neurosci* **10**, 325–339.

Hartveit E & Heggelund P (1993). The effect of acetylcholine on the visual response of lagged cells in the cat dorsal lateral geniculate nucleus. *Exp Brain Res* **95**, 443–449.

Hartveit E & Heggelund P (1995). Brainstem modulation of signal transmission through the cat dorsal lateral geniculate nucleus. *Exp Brain Res* **103**, 372–384.

Hartveit E, Ramberg SI & Heggelund P (1993). Brain stem modulation of spatial receptive field properties of single cells in the dorsal lateral geniculate nucleus of the cat. *J Neurophysiol* **70**, 1644–1655.

Heggelund P & Hartveit E (1990). Neurotransmitter receptors mediating excitatory input to cells in the cat lateral geniculate nucleus. I. Lagged cells. *J Neurophysiol* **63**, 1347–1360.

Hestrin S, Nicoll RA, Perkel DJ & Sah P (1990). Analysis of excitatory synaptic action in pyramidal cells using whole-cell recording from rat hippocampal slices. *J Physiol* **422**, 203–225.

Hirsch JC, Fourment A & Marc ME (1983). Sleep-related variations of membrane potential in the lateral geniculate body relay neurons of the cat. *Brain Res* **259**, 308–312.

Hubel DH (1960). Single unit activity in lateral geniculate body and optic tract of unrestrained cats. *J Physiol* **150**, 91–104.

Hubel DH & Wiesel TN (1961). Integrative action in the cat's lateral geniculate body. *J Physiol* **155**, 385–398.

Humphrey AL & Saul AB (1992). Action of brain stem reticular afferents on lagged and nonlagged cells in the lateral geniculate nucleus. *J Neurophysiol* **68**, 673–691.

Jacob V, Brasier DJ, Erchova I, Feldman D & Shulz DE (2007). Spike timing-dependent synaptic depression in the *in vivo* barrel cortex of the rat. *J Neurosci* **27**, 1271–1284.

Jahnsen H & Llinas R (1984*a*). Electrophysiological properties of guinea-pig thalamic neurons: an in vitro study. *J Physiol* **349**, 205–226.

Jahnsen H & Llinas R (1984*b*). Ionic basis for electroresponsiveness and oscillatory properties of guinea-pig thalamic neurons in vitro. *J Physiol* **349**, 227–247.

Kielland A & Heggelund P (2001). AMPA receptor properties at the synapse between retinal afferents and thalamocortical cells in the dorsal lateral geniculate nucleus of the rat. *Neurosci Lett* **316**, 59–62.

Kielland A & Heggelund P (2002). AMPA and NMDA currents show different short-term depression in the dorsal lateral geniculate nucleus of the rat. *J Physiol* **542**, 99–106.

Li B, Funke K, Wörgötter F & Eysel UT (1999). Correlated variations in EEG pattern and visual responsiveness of cat lateral geniculate relay cells. *J Physiol* **514**, 857–874.

Lindström S (1982). Synaptic organization of inhibitory pathways to principal cells in the lateral geniculate nucleus of the cat. *Brain Res* **234**, 447–453.

Lindström S & Wróbel A (1990). Frequency dependent corticofugal excitation of principal cells in the cat's dorsal lateral geniculate nucleus. *Exp Brain Res* **79**, 313–318.

Livingstone MS & Hubel DH (1981). Effects of sleep and arousal on the processing of visual information in the cat. *Nature* **291**, 554–561.

Mastronarde DN (1987*a*). Two classes of single-input X-cells in cat lateral geniculate nucleus. II. Retinal inputs and the generation of receptive-field properties. *J Neurophysiol* **57**, 381–413.

Mastronarde DN (1987*b*). Two classes of single-input X-cells in cat lateral geniculate nucleus. I. Receptive-field properties and classification of cells. *J Neurophysiol* **57**, 357–380.

Mayer ML, Westbrook GL & Guthrie PB (1984). Voltage-dependent block by Mg^{2+} and NMDA responses in spinal cord neurones. *Nature* **309**, 261–263.

McCormick DA (1992). Neurotransmitter actions in the thalamus and cerebral cortex and their role in neuromodulation and thalamocortical activity. *Prog Neurobiol* **39**, 337–388.

McCormick DA & Pape H-C (1990). Properties of a hyperpolarisation-activated cation current and its role in rhythmic oscillation in thalamic relay neurons. *J Physiol* **431**, 291–318.

Nowak L, Bregestovski P & Ascher P (1984). Magnesium gates glutamate-activated channels in mouse central neurones. *Nature* **307**, 462–465.

Perreault M-C, Quin Y, Heggelund P & Zhu JJ (2003). Postnatal development of GABAergic signalling in the rat lateral geniculate nucleus: presynaptic dendritic mechanisms. *J Physiol* **546**, 137–148.

Reinagel P & Reid RC (2000). Temporal coding of visual information in the thalamus. *J Neurosci* **20**, 5392–5400.

Reinagel P & Reid RC (2002). Precise firing events are conserved across neurons. *J Neurosci* **22**, 6837–6841.

Roy JP, Clerq M, Steriade M & Deschênes M (1984). Electrophysiology of neurons of the lateral thalamic nuclei of cat: mechanisms of long-lasting hyperpolarizations. *J Neurophysiol* **51**, 1220–1235.

Salt TE (1987). Excitatory amino acid receptors and synaptic transmission in the rat ventrobasal thalamus. *J Physiol* **391**, 499–510.

Sanchez JT, Gans D & Wenstrup JJ (2007). Contribution of NMDA and AMPA receptors to temporal patterning of auditory responses in the inferior colliculus. *J Neurosci* **27**, 1954–1963.

Scharfman HE, Lu SM, Guido W, Adams PR & Sherman SM (1990). N-Methyl-D-aspartate receptors contribute to excitatory postsynaptic potentials of cat lateral geniculate neurons recorded in thalamic slices. *Proc Natl Acad Sci U S A* **87**, 4548–4552.

Schuett S, Bonhoefer T & Hübener M (2001). Pairing-induced changes of orientation maps in cat visual cortex. *Neuron* **32**, 325–337.

Sheardown MJ, Nielsen EO, Hansen AJ, Jacobsen P & Honoré T (1990). 2,3-Dihydroxy-6-nitro-7-sulfamoyl-benzo(F)quinoxaline: a neuroprotectant for cerebral ischemia. *Science* **247**, 571–574.

Sillito AM, Murphy PC & Salt TE (1990*a*). The contribution of the non-N-methyl-D-aspartate group of excitatory amino-acid receptors to retinogeniculate transmission in the cat. *Neuroscience* **34**, 273–280.

Sillito AM, Murphy PC, Salt TE & Moody CI (1990*b*). Dependence of retinogeniculate transmission in cat on NMDA receptors. *J Neurophysiol* **63**, 347–355.

Soltesz I & Crunelli V (1992). $GABA_A$ and pre- and post-synaptic $GABA_B$ receptor mediated responses in the lateral geniculate nucleus. *Prog Brain Res* **90**, 151–169.

Steriade M & Deschênes M (1984). The thalamus as a neuronal oscillator. *Brain Res Rev* **8**, 1–63.

Steriade M, Jones EG & McCormick DA (1997). *Thalamus*. Elsevier Science, Oxford.

Stone C & Pinto LH (1992). Receptive field organization of retinal ganglion cells in the *spastic* mutant mouse. *J Physiol* **456**, 125–142.

Timofeev I, Contreras D & Steriade M (1996). Synaptic responsiveness of cortical and thalamic neurones during various phases of slow sleep oscillation in cat. *J Physiol* **494**, 265–278.

Turner JP, Leresche N, Guyon A, Soltesz I & Crunelli V (1994). Sensory Input and Burst Firing Output of Rat and Cat Thalamocortical Cells – the Role of Nmda and Non-Nmda Receptors. *J Physiol* **480**, 281–295.

Turner JP & Salt TE (1998). Characterization of sensory and corticothalamic excitatory inputs to rat thalamocortical neurones in vitro. *J Physiol* **510**, 829–843.

Usrey WM, Reppas JB & Reid RC (1997). Specificity and strength of retinogeniculate connections. *J Neurophysiol* **82**, 3527–3540.

von Krosigk M, Monckton JE, Reiner PB & McCormick DA (1999). Dynamic properties of corticothalamic excitatory postsynaptic potentials and thalamic reticular inhibitory postsynaptic potentials in thalamocortical neurons of the guinea-pig dorsal lateral geniculate nucleus. *Neuroscience* **91**, 7–20.

Zhang H & Kelly JB (2001). AMPA and NMDA receptors regulate responses of neurons in the rat's inferior colliculus. *J Neurophysiol* **86**, 871–880.

Zhu JJ, Lytton WW, Xue J-T & Uhlrich DJ (1999). An intrinsic oscillation in interneurons of the rat lateral geniculate nucleus. *J Neurophysiol* **81**, 702–711.

Acknowledgements

We are grateful to Dr Alan Saul for suggestions to improvements of the manuscript. The project was financially supported by the Norwegian Research Council.